

MR Molecular Imaging of Neovasculature May Predict Response to Antiangiogenic Therapy in Animal Cancer Models

A. H. Schmieder¹, P. M. Winter¹, T. A. Williams¹, J. S. Allen¹, G. Hu¹, H. Zhang¹, S. D. Caruthers^{1,2}, S. A. Wickline¹, and G. M. Lanza¹

¹Washington University School of Medicine, St Louis, MO, United States, ²Philips Medical Systems, Andover, MA, United States

Introduction:

Noninvasive high-resolution MR molecular imaging can provide a unique and powerful tool to characterize and quantify neovasculature in tumor models, which may be useful in stratifying tumor response to antiangiogenic therapies. In a Vx-2 adenocarcinoma model in rabbits, we have reported that $\alpha_v\beta_3$ -targeted fumagillin nanoparticles suppress the neovasculature and inhibit tumor growth. The objective of this study was to utilize MR molecular imaging and 3D neovascular mapping with $\alpha_5\beta_1$ -targeted fumagillin nanoparticles to quantify antiangiogenic and tumor growth responses to integrin targeted fumagillin nanoparticles in a xenograft tumor model.

Materials and Methods:

$\alpha_5\beta_1$ - or $\alpha_v\beta_3$ -targeted perfluorooctylbromide (PFOB) nanoparticles with fumagillin were made as previously published [1] using 2% (w/v) surfactant including 30 mole% Gd-DOTA-phosphatidylethanolamine (PE), 2mole% fumagillin, and 0.1 mole % of peptidomimetic $\alpha_5\beta_1$ -PEG-PE antagonist (IC₅₀ 0.39 nM) or $\alpha_v\beta_3$ -PEG-PE particles (IC₅₀ ~ 50nM). The $\alpha_v\beta_3$ peptidomimetic has no significant integrin cross-reactivity while the $\alpha_5\beta_1$ antagonist also binds $\alpha_v\beta_3$ -integrin (IC₅₀ 87nM). Nude mice implanted with human MDA435 cells were dosed with $\alpha_v\beta_3$ -targeted fumagillin nanoparticles (n=5), $\alpha_5\beta_1$ -targeted fumagillin nanoparticles (n=5), or saline (n=4) on days 7, 11, 15, and 19 post implantation. On day 22, tumor volume and neovascularity was assessed in all animals by MR molecular imaging with $\alpha_5\beta_1$ -targeted paramagnetic nanoparticles. MR images (Philips Achieva, 3T) were acquired at baseline and 120 min post injection using 3D T1w fat suppressed gradient echo images (FOV 100mm, 0.5 mm slices, 256x256 matrix, TR/TE = 46/3.9 ms, 40° flip angle) obtained with a SENSE-Flex-M coil. At 120 minutes, enhancing MRI pixels were selected based on a threshold equal to three times the standard deviation of the tumor signal at baseline, and the percent of the total tumor volume enhancing was calculated. Three-dimensional reconstructions of tumor signal enhancement were created using MATLAB.

Results and Discussion

3D MR molecular imaging of targeted angiogenesis in mice implanted with MDA435 tumors was substantially lower and sparser than the neovascularity previously observed in Vx2 rabbits. $\alpha_5\beta_1$ -fumagillin-nanoparticles decreased ($p < 0.05$) angiogenesis relative to control tumors ($1.3 \pm 0.3\%$ of the peripheral tumor volume) to an almost negligible level ($0.5 \pm 0.3\%$) when characterized at 22d with $\alpha_5\beta_1$ -paramagnetic-nanoparticles (Fig 1). Unexpectedly, serial treatment with $\alpha_v\beta_3$ -fumagillin-nanoparticles did not decrease ($p > 0.05$) angiogenesis relative to control at 22d ($1.0 \pm 0.3\%$). The differential angiogenic response suggests that the cross-reactive $\alpha_5\beta_1$ -ligand either reaches a subset of neovessels that are not targeted with $\alpha_v\beta_3$ alone, or that the dual targeting of both integrins increased delivery of fumagillin to cells, which improved antiangiogenic efficacy. Nevertheless, neither treatment regimen affected tumor volume, which suggests that xenograft tumor growth is largely independent of angiogenesis (Fig 2). Although diminished angiogenesis was observed with integrin-targeted fumagillin in the previous Vx2 and current mouse MDA 435 xenograft model, tumor growth reduction was observed only in rabbit adenocarcinoma, which exhibited an “angiogenic switch” phenotype and rapid tumor growth.

Conclusion:

Neovascularity of MDA435 xenograft mice was low and further decreased with $\alpha_5\beta_1$ -targeted but not $\alpha_v\beta_3$ -targeted antiangiogenic treatment. However, MDA435 tumor size was unaffected by either regimen, suggesting that MDA435 xenograft tumor growth has little dependence on angiogenesis, unlike previous results in the rabbit Vx2 model. These data illustrate the prognostic opportunities afforded by noninvasive high-resolution MR molecular imaging. Characterizing and quantifying tumors with regard to neovascular status may be clinically relevant in establishing personalized therapy regimens.

References 1.Schmieder, et al. Magn Reson Med, 2005.

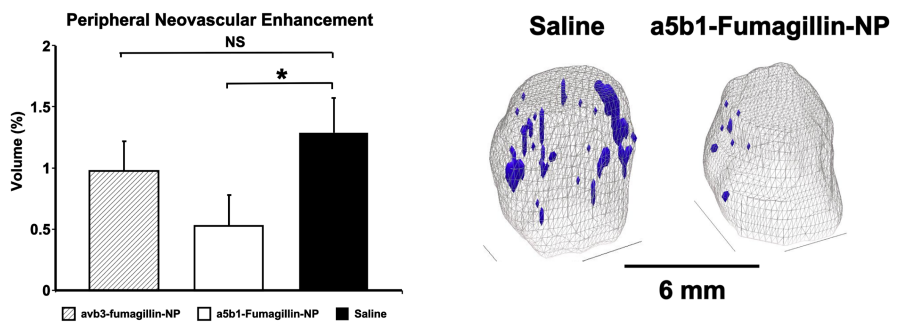


Fig 1. Left, Histogram revealing the extent of neovascularity as a percent of the tumor peripheral volume interrogated with $\alpha_5\beta_1$ -paramagnetic-nanoparticles. Right, 3D neovascular maps of 22d tumors treated with $\alpha_5\beta_1$ -fumagillin-nanoparticles versus saline control.

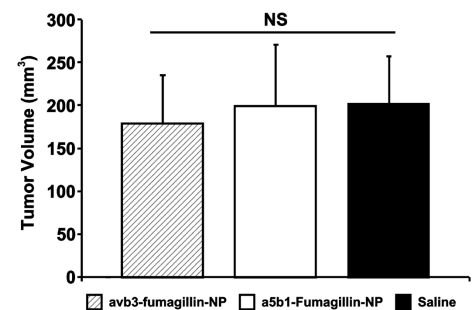


Fig. 2 Integrin-targeted fumagillin had no effect on tumor volume in the MDA435 xenograft model